CELL REGULATION, Vol. 1, 951–963, November 1990

Simultaneous analysis of cell Ca^{2+} and Ca^{2+}-stimulated chloride conductance in colonic epithelial cells (HT-29)

Andrew P. Morris,* Kevin L. Kirk, and Raymond A. Frizzell
Department of Physiology and Biophysics
University of Alabama at Birmingham
Birmingham, Alabama 35294

We used perforated patch, whole-cell current recordings and video-based fluorescence ratio imaging to monitor the relation of plasma membrane ionic conductances to intracellular free Ca^{2+} within individual colonic epithelial cells (HT-29). The Ca^{2+}-mediated agonist, neurotensin, activated K^+ and Cl^- conductances that showed different sensitivities to $[Ca^{2+}]_i$. The Cl^- conductance was sensitive to increases or decreases in $[Ca^{2+}]_i$ around the resting value of 76 ± 32 (mean ± SD) nM (n = 46), whereas activation of the K^+ conductance required at least a 10-fold rise in $[Ca^{2+}]_i$. Neurotensin increased $[Ca^{2+}]_i$ by stimulating a transient intracellular Ca^{2+} release, which was followed by a sustained rise in $[Ca^{2+}]_i$ due to Ca^{2+} influx from the bath. The onset of the initial $[Ca^{2+}]_i$ transient, monitored at a measurement window over the cell interior, lagged behind the rise in Cl^- current during agonist stimulation. This lag was not present when the $[Ca^{2+}]_i$ rise was due to Ca^{2+} entry from the bath, induced either by the agonist or by the Ca^{2+} ionophore ionomycin. The temporal differences in $[Ca^{2+}]_i$ and Cl^- current during the agonist-induced $[Ca^{2+}]_i$ transient can be explained by a localized Ca^{2+} release from intracellular stores in the vicinity of the plasma membrane Cl^- channel. Chloride currents recover toward basal values more rapidly than $[Ca^{2+}]_i$ after the agonist-induced $[Ca^{2+}]_i$ transient, and, during a sustained neurotensin-induced $[Ca^{2+}]_i$ rise, Cl^- currents inactivate. These findings suggest that an inhibitory pathway limits the increase in Cl^- conductance that can be evoked by agonist. Because this Cl^- current inhibition is not observed during a sustained $[Ca^{2+}]_i$ rise induced by ionomycin, the inhibitory pathway may be mediated by another agonist-induced messenger, such as diacylglycerol.

* Corresponding author.

Introduction

Electrolyte and fluid secretion across mammalian intestine is driven by a secondary-active Cl^- transport process (Frizzell *et al.,* 1979). Chloride is accumulated by secretory cells because of the combined actions of three basolateral membrane transport mechanisms: $Na^+/K^+/Cl^-$ co-transport, Na^+/K^+ pump, and K^+ channels. Chloride exits across the apical membrane down its electrochemical gradient via apical Cl^- channels. Signal transduction pathways involving cyclic adenosine monophosphate (cAMP), cyclic guanosine monophosphate (cGMP), and Ca^{2+} mediate the secretory actions of various neurohumoral agents by activating one or more of these transport mechanisms (Halm and Frizzell, 1990). However, it is generally agreed that these regulatory pathways converge on the apical membrane Cl^- conductance, the activation of which is a necessary feature of the secretory response (Frizzell and Halm, 1990).

Transepithelial measurements have shown that Ca^{2+} ionophores and Ca^{2+}-mediated agonists stimulate transepithelial Cl^- transport, yet little is known of the relation of the intracellular free Ca^{2+} concentration, $[Ca^{2+}]_i$, to membrane Cl^- conductance. Transepithelial Cl^- secretion is conveniently monitored in Ussing chambers by the use of intestinal sheets or monolayers of cultured cell lines. However, $[Ca^{2+}]_i$ has rarely been determined with similar preparations (Wong *et al.,* 1989), and the results of several studies have raised doubts as to whether Ca^{2+} activates Cl^- conductance pathways, or whether its effects are mediated via generation of other second messengers (Smith and McCabe, 1984; Reinlib *et al.,* 1989) or by stimulation of other Ca^{2+}-dependent transport events (Dharmsathaphorn *et al.,* 1989).

To establish calcium's role as a mediator of Cl^- conductance changes during secretion, and as a first approach to resolution of the regulatory proteins involved in mediating the effects of Ca^{2+}, we examined, simultaneously, the temporal relations between changes in Cl^- conductance and $[Ca^{2+}]_i$ during agonist activation.

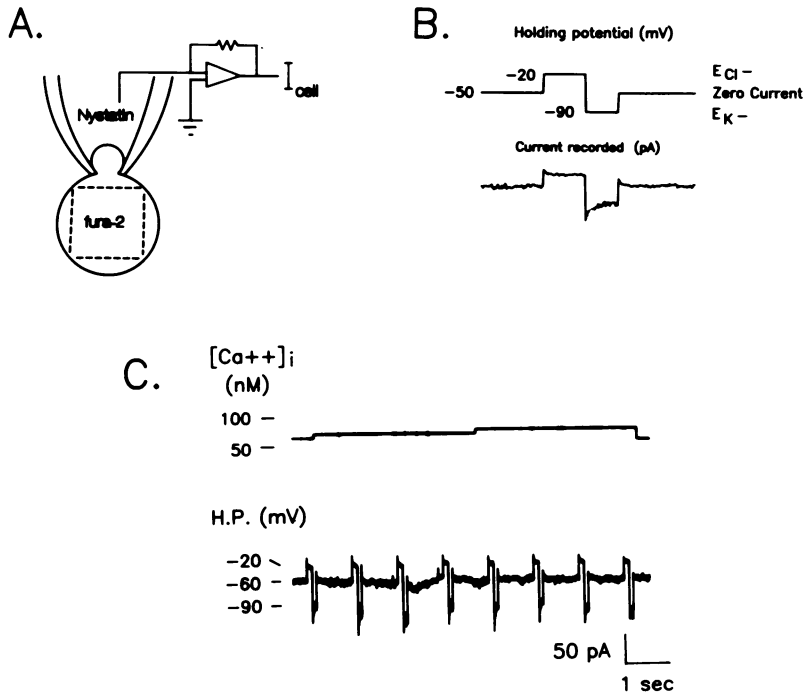

***Figure 1.* Simultaneous whole-cell current and calcium measurements.** (A) Perforated patch whole-cell current recordings were obtained by including nystatin (100 μg/ml) in the recording pipette. The dashed lines indicate the approximate relation of the fluorescence measurement window to the cell's boundaries. (B) Cells were voltage-clamped to three holding potentials (H.P.): (a) −20 mV = E_{Cl^-}, (b) −90 mV = E_{K^+}, and (c) the zero-current voltage recorded in the absence of agonist; the lower trace shows currents recorded at each H.P. (C) Expanded time scale showing relations between current and $[Ca^{2+}]_i$ measurements from the same cell. Four voltage-clamp cycles were run during the time for a single calcium measurement (3.7 s). In subsequent experimental records, the voltage-clamp values (H.P.) are provided at the left of each current trace, as shown. Individual current pulses are often obscured because of time compression of the records.

Chloride-selective conductance pathways were isolated using perforated patch, whole-cell recording; $[Ca^{2+}]_i$ was monitored using the Ca^{2+} fluorophore fura-2. These methods were applied to the colonic tumor cell line HT-29, first isolated by Fogh (Fogh and Trempe, 1975). In their undifferentiated form, HT-29 cells express receptors for the Ca^{2+}-mediated agonists carbachol (Kopp *et al.,* 1989) and neurotensin (Kitabgi *et al.,* 1980), which have been shown to activate inositol polyphosphate hydrolysis and cellular Ca^{2+} mobilization in cells in suspension (Turner and Bollinger, 1989). Thus, HT-29 cells serve as a model for the Ca^{2+}-mediated regulatory events that activate Cl^- secretion by intestinal cells and other Cl^--secreting epithelia.

Results

Simultaneous whole-cell current and cell Ca^{2+} recordings in HT-29 cells

The ionic conductances of individual HT-29 cells were measured with the whole-cell, voltage-clamp recording technique (Hamill *et al.,* 1981). $[Ca^{2+}]_i$ was determined from the fluorescence of fura-2 (Grynkiewicz *et al.,* 1985), loaded in its esterified form, fura-2/AM. However, during conventional whole-cell recording, dialysis of the cell cytoplasm by the pipette solution resulted in loss of cellular fura-2 fluorescence. Conversely, if the pipette was loaded with the unesterified dye, measurement of $[Ca^{2+}]_i$ was compromised by stray fluorescence from the dye-filled pipette. To overcome these problems, we used the perforated-patch method of Horn and Marty (1988), which allowed for measurement of whole-cell currents without significant loss of cellular dye fluorescence. A low cellular access resistance was obtained by adding nystatin (100 μg/ml) to the pipette solution (Figure 1A). Stable cellular resistance and capacitance levels were obtained within minutes after making the gigaseal.

Whole-cell currents. Individual ionic conductances were monitored by recording the currents evoked at two clamp voltages, chosen to correspond to the calculated Nernst equilibrium potentials (E_{ion}) for K^+ (−90 mV) and Cl^- (−20 mV) (Figure 1B). The currents monitored at these voltages represent inward Cl^- and outward K^+ currents, respectively. The current clamp voltage (I = 0) was employed as the holding potential. As shown in Figure 1C, approximately four current pulses were recorded during a single $[Ca^{2+}]_i$ determination. Therefore, the time of onset of cellular responses to agonists was taken from the changes in membrane current, which were better resolved in time than the $[Ca^{2+}]_i$ values.

A convenient measure of cell conductance was the change in current needed to voltage clamp between E_{Cl^-} and E_{K^+}, which we will refer

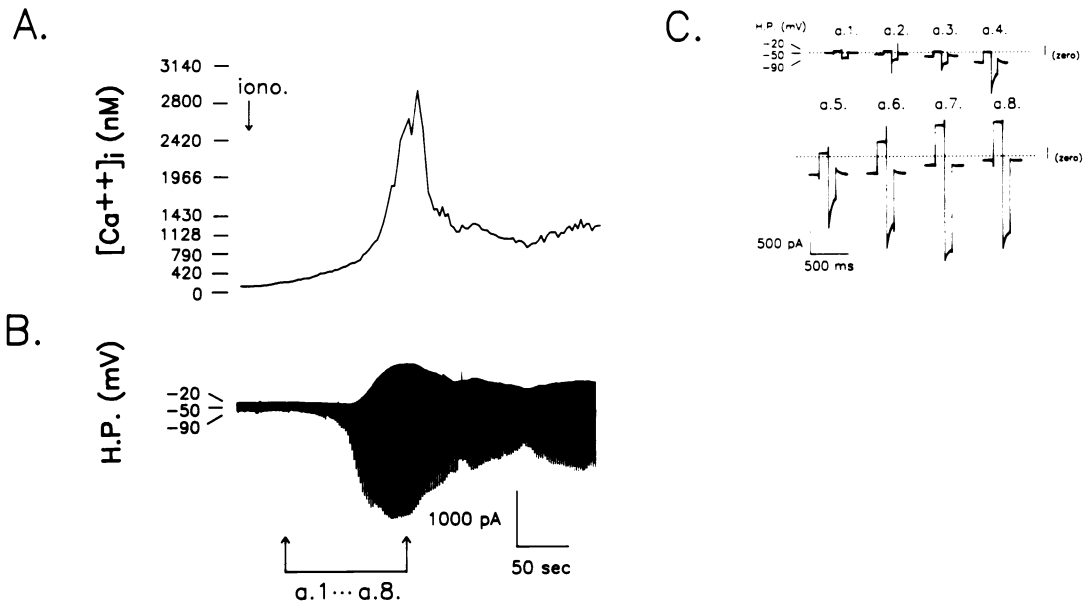

Figure 2. **Effect of calcium ionophore on $[Ca^{2+}]_i$ and whole-cell currents.** (A) Simultaneous $[Ca^{2+}]_i$ and (B) whole-cell currents, recorded after addition of 10^{-6} M ionomycin (iono.) to the standard bath containing 1 mM $[Ca^{2+}]_o$. Inward Cl^- currents are measured at E_{K^+} (−90 mV); outward K^+ currents are measured at E_{Cl^-} (−20 mV). (C) Currents recorded at 15-s intervals during the $[Ca^{2+}]_i$ rise to peak values (a1 · · · a8 in 2B).

to as the whole-cell current amplitude ($\Delta I_{-20,-90}$). In resting cells, $\Delta I_{-20,-90}$ was similar with the use of the perforated patch (76 ± 27 [mean ± SD] pA, n = 25) and the conventional whole-cell methods (72 ± 20 pA, n = 5). The conventional whole-cell measurements were obtained with 0.1–0.5 mM ethylene glycol-bis(β-aminoethyl ether)-*N,N,N′,N′*-tetraacetic acid (EGTA) and no added calcium in the pipette solution.

Intracellular Ca^{2+} measurements. In most experiments, $[Ca^{2+}]_i$ was monitored as the mean fluorescence intensity within a square measurement window placed within the cell's fluorescence image (– – –, Figure 1A). This provides a measure of the generalized cellular $[Ca^{2+}]_i$, with which the whole-cell currents were compared. In ratio-imaged, fura-2 loaded cells under resting conditions, cell Ca^{2+} was 73 ± 29 (mean ± SD) nM (n = 51). When ratio-imaging was combined with simultaneous whole-cell current recording, resting $[Ca^{2+}]_i$ levels averaged 76 ± 32 nM (n = 46). The current clamp voltage of fura-2 loaded cells yielded a mean resting membrane potential (E_m) of −39 ± 5 (mean ± SD) mV (n = 46), similar to the E_m found in cells not preloaded with fura-2 (−38 ± −2.8 mV, n = 5). Voltage clamping the membrane potential over a wide range (−90 mV–+50 mV) had no effect on $[Ca^{2+}]_i$, demonstrating that voltage-dependent calcium mobilization pathways are absent.

Ionophore-induced changes in $[Ca^{2+}]_i$ and whole-cell currents

The calcium ionophore ionomycin was used to elevate $[Ca^{2+}]_i$ artificially as an initial step in characterizing the relation of membrane conductances to $[Ca^{2+}]_i$. Ionophore-induced currents monitored by the conventional whole-cell method (n = 5) were indistinguishable from those obtained with the nystatin pipette technique. Addition of ionomycin (1 μM) under standard conditions ($[Ca^{2+}]_o$ = 1 mM) elicited large and sustained rises in whole-cell currents: $\Delta I_{-20,-90}$ rose >10-fold to 1140 ± 460 pA (n = 15). This coincided with large, sustained rises in $[Ca^{2+}]_i$ when simultaneous ratio-imaging was performed (n = 12).

Figure 2 shows representative tracings of simultaneously determined whole-cell currents and $[Ca^{2+}]_i$ during stimulation by ionomycin. The ionophore-induced Ca^{2+} rise peaked at 3 μM before a sustained level of ~1 μM was obtained. The transient peak in $[Ca^{2+}]_i$ probably reflects release of stored calcium in combination with an ionomycin-induced calcium influx from the bath. The whole-cell current amplitude follows $[Ca^{2+}]_i$ closely, particularly at elevated (>1 μM) Ca^{2+} levels. As shown by the expanded current tracings (Figure 2C), the activation of outward current at E_{Cl^-} (−20 mV) initially lagged behind the increase in inward current recorded at E_{K^+}

(−90 mV) (Figure 2C, a1 · · · a4). The mean lag time was 10 ± 15 (SD) s (n = 12). Thus, the initial $[Ca^{2+}]_i$ rise acted predominantly to increase inward Cl^- current without increasing outward K^+ current (n = 16). This was confirmed by the development of net inward current at the holding potential of −50 mV (formerly the zero-current level in the absence of agonist) and by the agreement between E_{Cl^-} and the zero-current level during this period (a2 · · · a4). Generation of an outward K^+ current required a substantial $[Ca^{2+}]_i$ rise (Figure 2, A and B). Comparison of the time courses of $[Ca^{2+}]_i$ and outward current provided an estimate of the $[Ca^{2+}]_i$ level required to increase I_{K^+} of 772 ± 308 nM (n = 16). As predicted from the delayed increase in K^+ conductance, the current monitored at −50 mV recovered toward its original zero-current level as the outward K^+ current increased (a4 · · · a8).

Currents recorded at E_{K^+} and E_{Cl^-} peaked together with the corresponding peak $[Ca^{2+}]_i$ rise (Figure 2, A and B). On an expanded time scale (Figure 2C), the Cl^- currents recorded during voltage pulses to −90 mV displayed a characteristic time-dependent relaxation to a lower steady-state level. These relaxations could be fit with a single exponential (time constant = 346 ± 31 [mean ± SD] ms, n = 6), which was not particularly affected by the current amplitude. The sustained effects of ionomycin on whole-cell currents and $[Ca^{2+}]_i$ were freely reversible on washout of the ionophore (n = 6) and/or by replacement of the bath solution with one containing no added calcium and 1 mM EGTA (n = 6).

When cell membrane potential was recorded in the current-clamp mode, ionomycin induced a depolarization to −15.5 ± 5 mV (n = 12). This value is slightly positive to the E_{Cl^-} calculated from our bath and pipette Cl^- concentrations (−20 mV), and possible sources of this discrepancy will be discussed below. The peak depolarization of E_m coincided with the peak of $[Ca^{2+}]_i$, and E_m returned to its resting value only after $[Ca^{2+}]_i$ returned to control levels.

Calcium sensitivity of the basal whole-cell current

When 1 μM ionomycin was added to a Ca^{2+}-free bath (no added calcium, 1 mM EGTA), the $[Ca^{2+}]_i$ and current responses were biphasic. Initially, ionomycin induced simultaneous increases in whole-cell currents and $[Ca^{2+}]_i$, resulting from release of intracellular Ca^{2+} stores. This was followed by decreases in current and $[Ca^{2+}]_i$ to below resting levels (n = 9). $\Delta I_{-20,-90}$, after depletion of cell calcium, was reduced to 47 ± 15 pA, and at this time $[Ca^{2+}]_i$ was 32 ± 17 nM (n = 9). In three experiments where the ionophore-induced calcium release was sufficient to activate current at both E_{Cl^-} and E_{K^+}, recovery of the K^+ current preceded that of Cl^-, again demonstrating the greater sensitivity of the Cl^- conductance to $[Ca^{2+}]_i$.

Current-clamp recordings from ionophore-treated cells under Ca^{2+}-free conditions showed a steady-state hyperpolarization of the membrane potential (ΔE_m = −21 ± 5 mV [n = 7]), suggesting that Cl^- conductance decreased during cell Ca^{2+} depletion. These findings demonstrate that the current monitored under resting conditions is sensitive to changes in $[Ca^{2+}]_i$ in both directions from the basal level of ~75 nM. Because of the sensitivity of the cellular Cl^- current to $[Ca^{2+}]_i$, the Ca^{2+}-dependent control of E_m is exerted predominantly through changes in cellular Cl^- conductance.

Effects of agonists on whole-cell currents and $[Ca^{2+}]_i$

Addition of the peptide agonist neurotensin to the bathing media activated whole-cell currents and elevated cell Ca^{2+}. Simultaneous recording of $[Ca^{2+}]_i$ and whole-cell currents (Figure 3) showed that agonist effects were transient and consisted of several phases. The peak $[Ca^{2+}]_i$ was similar whether measured by either imaging alone or imaging together with whole-cell current recording: 1000 ± 790 nM (n = 33) and 1210 ± 860 nM (n = 28), respectively. At the peak of stimulation, neurotensin induced a 10-fold increase in $\Delta I_{-20,-90}$ to 746 ± 616 pA.

In most cases (18/26), neurotensin activated inward Cl^- current alone, with no stimulation of outward K^+ current (Figure 3B). As observed during stimulation by ionomycin, the activation of K^+ conductance required a $[Ca^{2+}]_i$ rise to levels > ~800 nM (n = 5). Agonist-induced increases in whole-cell current and $[Ca^{2+}]_i$ were often followed by rapid decreases in both parameters to below resting levels (Figure 3, Ai and Bi). This was followed by a gradual rise in both current and $[Ca^{2+}]_i$ to sustained levels that exceeded those before agonist addition.

Figure 3C provides a cellular $[Ca^{2+}]_i$ map during each phase of the response to neurotensin. Before the onset of agonist effects (0 s), $[Ca^{2+}]_i$ was uniformly distributed at resting values across the entire cell. At a time near the peak Ca^{2+} rise (7 s), $[Ca^{2+}]_i$ was elevated in the cytoplasm. Subsequently (58 s), $[Ca^{2+}]_i$ fell to below resting levels and then rose during the sus-

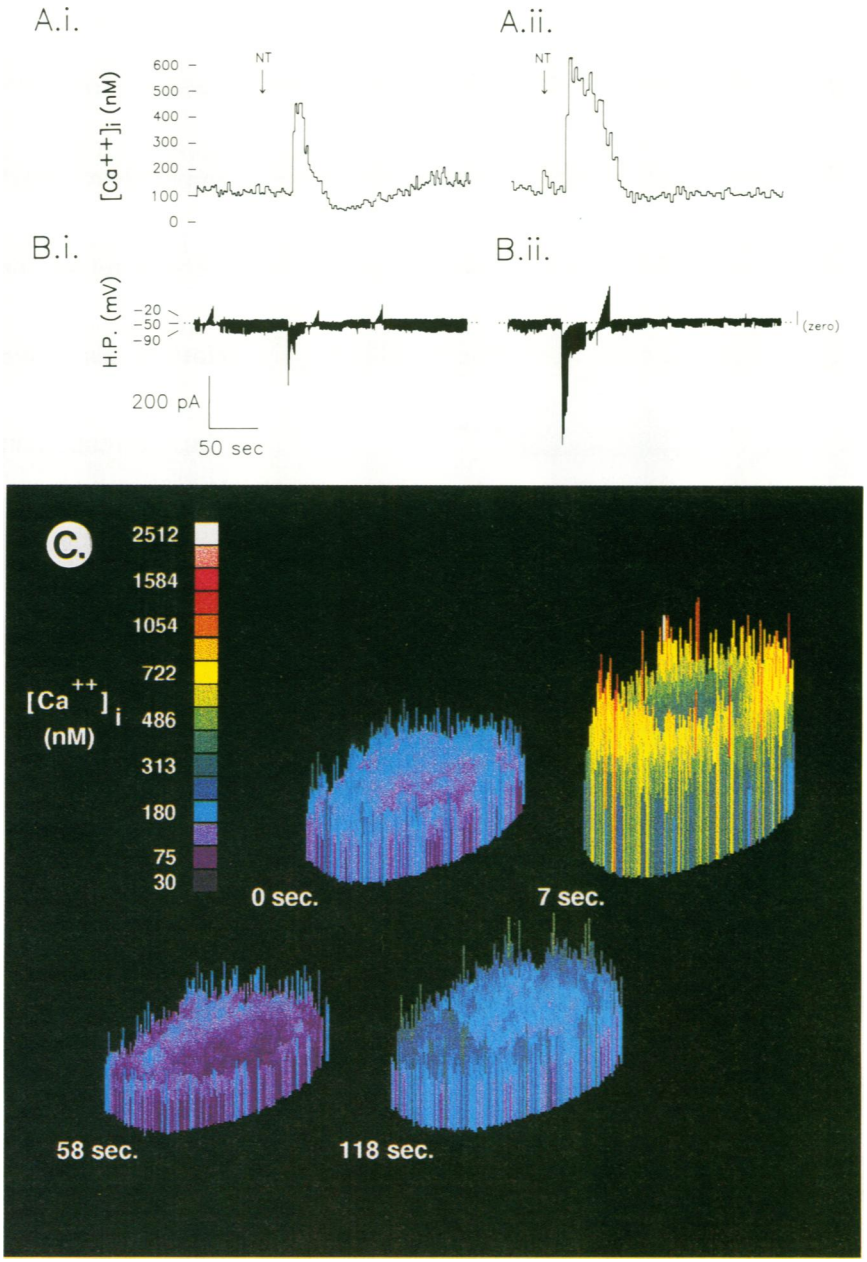

Figure 3. **Effect of neurotensin on $[Ca^{2+}]_i$ and whole-cell currents.** Neurotensin (NT, 5×10^{-8} M) was added to the standard bath (1 mM $[Ca^{2+}]_o$) during (A) $[Ca^{2+}]_i$ and (B) whole-cell current determinations from a single cell at two times (i and ii) separated by 30 min. The first addition was made shortly after fura-2 loading and washout of esterified dye. The periods during which the continuous pulse record is disrupted represent the acquisition of current-voltage relationships (see below). The lag between addition of agonist and onset of the $[Ca^{2+}]_i$ and current responses is due to perfusion system delay. (C) Image map of $[Ca^{2+}]_i$ during the neurotensin response. Whole-cell currents were also monitored (not shown). Individual pixels within the cell were false-colored according to calibrated $[Ca^{2+}]_i$ values (displayed on a pseudocolor scale at the right). $[Ca^{2+}]_i$ was imaged before the onset of stimulation (0 s), during the peak $[Ca^{2+}]_i$ (7 s), during the recovery below resting $[Ca^{2+}]_i$ (58 s), and during the subsequent sustained $[Ca^{2+}]_i$ rise (118 s).

tained phase of stimulation (118 s) to an elevated steady-state concentration. At these later times, the $[Ca^{2+}]_i$ distribution was fairly uniform. The inhomogeneity of $[Ca^{2+}]_i$ observed during the Ca^{2+} transient (7 s) will be discussed below, where the temporal relations between $[Ca^{2+}]_i$ and Cl^- current are considered.

Repetitive agonist stimulation of the same cell did not always reproduce all of these phases of Ca^{2+} mobilization. As shown in Figure 3, Aii and Bii, addition of agonist to the same cell 30 min later elicited a larger $[Ca^{2+}]_i$ response, which recovered more slowly from its peak value. No undershoot to a lower-than-resting $[Ca^{2+}]_i$ was seen. Associated with this larger Ca^{2+} rise was a larger peak inward current; however, the duration of current stimulation was not prolonged. No clear relationship existed between starting values of $[Ca^{2+}]_i$ and the peak responses of $[Ca^{2+}]_i$ or current.

In a small proportion of cells (3/19), neurotensin elicited large rises in $[Ca^{2+}]_i$. As illustrated in Figure 4, the $[Ca^{2+}]_i$ rise was sufficient to activate K^+ current after the Cl^- current had

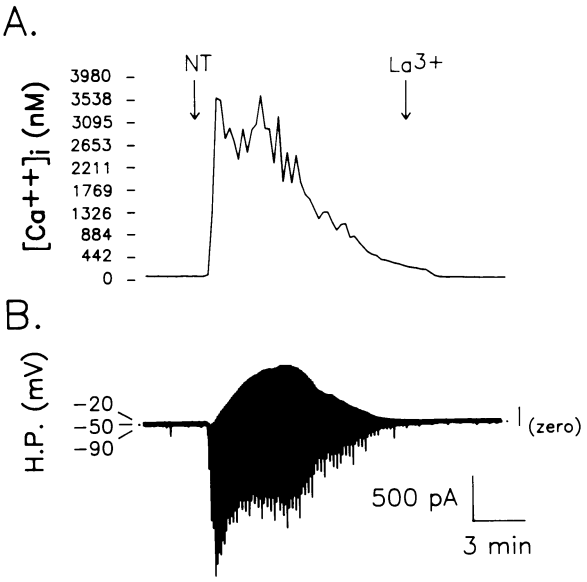

Figure 4. **Large current and $[Ca^{2+}]_i$ responses in a neurotensin-stimulated cell.** Conditions as in Figure 3; 10^{-4} M $[La^{3+}]_o$ added at time shown.

peaked. Significant inactivation of the inward Cl^- current was seen in all three experiments during these prolonged $[Ca^{2+}]_i$ rises. However, ionophore-induced $[Ca^{2+}]_i$ levels of a similar magnitude did not lead to a rapid inactivation of Cl^- current (see Figure 2). This lack of direct proportionality between Cl^- current and $[Ca^{2+}]_i$ during the response to agonist implies that factors other than Ca^{2+} control the Cl^- conductance (see below). In contrast, the outward K^+ current induced by either ionophore or agonist did not show inactivation during prolonged $[Ca^{2+}]_i$ rises (Figures 2 and 4).

Na^+-free bath. When outward K^+ current stimulation was absent, a transient inward current was often recorded at the E_{Cl^-} (−20 mV), suggesting that Ca^{2+} stimulated an inward cation current (e.g., compare Figures 3 and 4). However, the inward current transient at E_{Cl^-} was not affected by removal of extracellular Ca^{2+} or Na^+ (*N*-methyl-D-glucamine replacement [NMDG], data not shown). The transient inward current at E_{Cl^-} may result from a lack of complete equilibration of cell and pipette Cl^- during the initial phase of stimulation. Cell $[Cl^-]$ could be higher for a brief period than pipette $[Cl^-]$. As discussed above, shifts in the current-clamp voltage suggest that the reversal potential of this current transient is −15 mV, which would be consistent with a transient increase in cell $[Cl^-]$ from 60 to 80 mM.

Properties of the Ca^{2+}-induced Cl^- current

Whole-cell currents were recorded at two steady-state $[Ca^{2+}]_i$ levels (Figure 5). At $[Ca^{2+}]_i$ = 95 nM, clamping the membrane potential between −90 and +50 mV elicited a total current amplitude of 150 pA. A rise in $[Ca^{2+}]_i$ to 360 nM elicited 950 pA of outwardly-rectified Cl^- current. The current recorded at −90 mV displays a characteristic time-dependent relaxation (as in Figure 2), and that recorded at +50 mV shows a time-dependent increase in current to steady-state levels. These properties are similar to those of the Ca^{2+}-stimulated Cl^- current in the T84 colonic cell line (Cliff and Frizzell, 1990). The corresponding current-voltage relationships are plotted in Figure 5B. On elevation of $[Ca^{2+}]_i$, the zero-current potential shifted from −60 mV to a more depolarized value; both instantaneous and steady-state currents reversed near the E_{Cl^-} (−20 mV). The Ca^{2+}-activated Cl^- currents show greater outward rectification at steady-state because of the time-dependence of the currents at depolarizing and hyperpolarizing voltages.

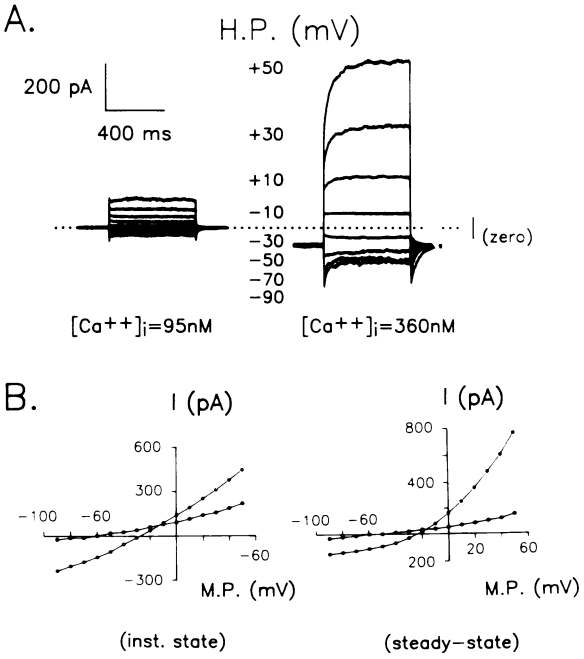

Figure 5. **Current-voltage relations at two $[Ca^{2+}]_i$ values.** (A) Overlay of Cl^- currents recorded during voltage pulses from −90 mV to +50 mV (20-mV increments) at $[Ca^{2+}]_i$ levels of 95 and 360 nM in the same cell bathed by Na^+-free solutions. Voltage pulses were of 0.5-s duration and separated by a 0.5-s interval at −40 mV. (B) Current-voltage relations obtained at $[Ca^{2+}]_i$ = 95 nM (●) and $[Ca^{2+}]_i$ = 360 nM (○). Instantaneous currents were recorded 7 ms after the onset of the voltage pulse and steady-state currents at 400 ms.

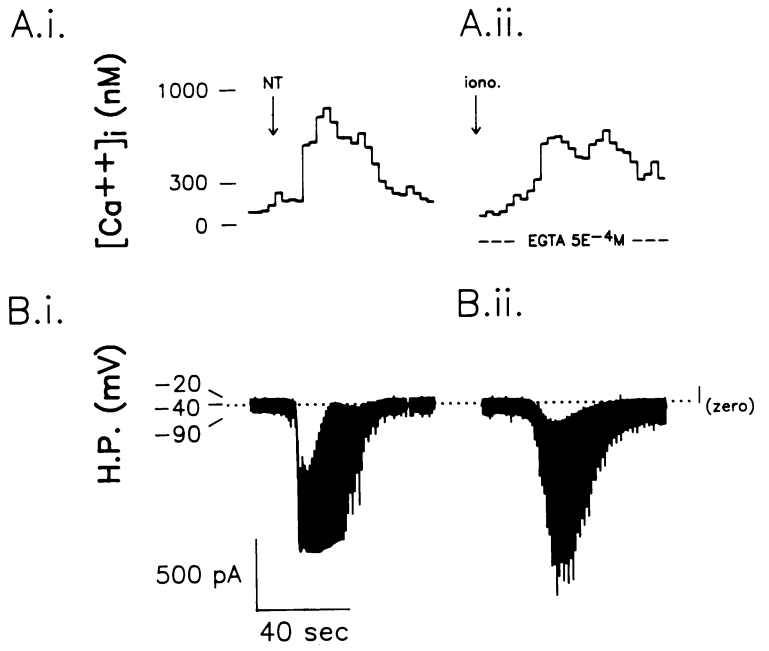

Figure 6. **Effects of neurotensin and ionomycin on $[Ca^{2+}]_i$ and whole-cell currents.** Neurotensin (5×10^{-8} M) and ionomycin (10^{-6} M) were added to the same cell at the times shown. NT was added to standard 1-mM $[Ca^{2+}]_o$ bath and washed out after record i was obtained; record ii was obtained 5 min later, 2 min after the bath was replaced by a Ca^{2+}-free medium containing 5×10^{-4} M EGTA.

Temporal relations between $[Ca^{2+}]_i$ and Cl^- currents in agonist-stimulated cells

These simultaneous measurements of $[Ca^{2+}]_i$ and whole-cell current make possible a close temporal comparison of the Cl^- current and Ca^{2+} responses to neurotensin. The time to peak inward current averaged 3.5 ± 1.8 s, and the duration of the agonist-induced current response was 42.4 ± 19 s (n = 19). The $[Ca^{2+}]_i$ response peaked later, at 6.7 ± 2.7 s, and the duration of the $[Ca^{2+}]_i$ transient was longer and more variable at 66 ± 77 s (paired means, n = 19). Thus, when measured from the onset of the Cl^- current rise, the peak $[Ca^{2+}]_i$ transient occurred, on average, 3.2 s later than the peak Cl^- current. At the $[Ca^{2+}]_i$ peak, the Cl^- current had already inactivated to 65 ± 19% (mean ± SD) of its peak value (n = 19).

Figure 6 illustrates this lack of strict temporal correlation between Cl^- current and $[Ca^{2+}]_i$ during the initiation of the response to neurotensin (Figure 6, Ai and Bi). Addition of ionomycin to the same cell in the absence of bath Ca^{2+} (1 mM EGTA, no added calcium) also evoked a transient increase in inward Cl^- current (Figure 6, Aii and Bii), but the initial rise in current coincided well with the ionophore-induced $[Ca^{2+}]_i$ rise.

Cell Ca^{2+} levels recorded throughout this study were monitored as the average $[Ca^{2+}]_i$ within a measurement window with boundaries within the cellular fluorescence image (Figure 1A). To test whether spatial differences in $[Ca^{2+}]_i$ could explain the discrepancy between the initial current and $[Ca^{2+}]_i$ time-courses, 1,2-bis-(2-aminophenoxy)ethane-N,N,N′,N′-tetra acetic acid (BAPTA) was used as a cell Ca^{2+} buffer to slow Ca^{2+} diffusion through the cytoplasm and magnify differences between the current and $[Ca^{2+}]_i$ responses. Cells were loaded by exposure to BAPTA/AM during fura-2 loading, and $[Ca^{2+}]_i$ levels were monitored both at the periphery and interior of BAPTA- and fura-2–loaded cells. BAPTA loading prevented the activations of whole-cell current and $[Ca^{2+}]_i$ by neurotensin (5×10^{-8} M) (n = 24).

As shown in Figure 7, treatment of BAPTA-loaded cells with ionomycin (1 μM) elicited sluggish rises in both whole-cell current and $[Ca^{2+}]_i$, indicating that the effects of BAPTA are due to chelation of cell Ca^{2+}. BAPTA introduced a lag of 240 ± 60 s (n = 3) between current activation and the $[Ca^{2+}]_i$ rise monitored in the center of the cell. In contrast, $[Ca^{2+}]_i$ monitored at the plasma membrane (Figure 8A.2) paralleled the changes in whole-cell current (Figure 8B). $[Ca^{2+}]_i$ peaked at similar values in both the center and periphery. Subsequent chelation of extracellular calcium (1 mM EGTA bath) in the continued presence of ionophore returned both $[Ca^{2+}]_i$ and whole-cell currents toward resting values. The close correlation between Cl^- current and Ca^{2+} at the plasma membrane suggests that the discrepancies between $[Ca^{2+}]_i$ and Cl^- current during stimulation by neurotensin result from spatial inhomogeneities in cell Ca^{2+}.

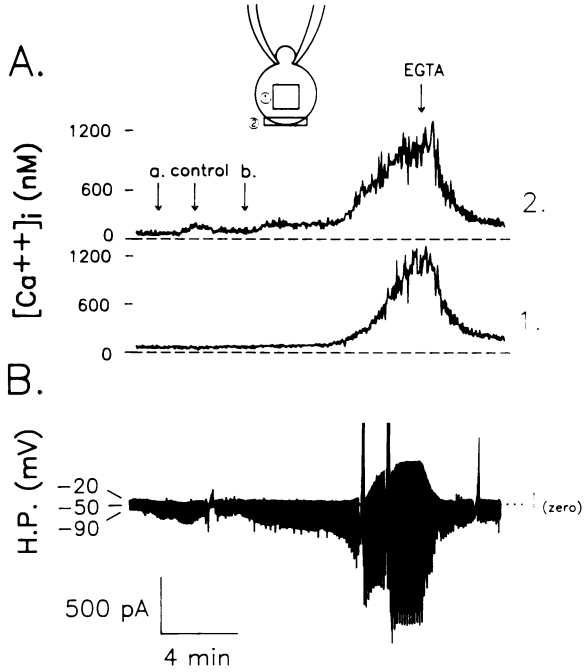

Figure 7. **Effect of ionomycin on $[Ca^{2+}]_i$ and whole-cell currents in a BAPTA-loaded cell.** (A) The calcium chelator BAPTA/AM (10 μM) was loaded together with fura-2/AM and $[Ca^{2+}]_i$ monitored at the center (A.1) and periphery (A.2). (B) Corresponding whole-cell currents during perfusion of the bath with the standard solution (1 mM $[Ca^{2+}]_o$) containing ionomycin; (a) 0.5 μM; (b) 1 μM; at EGTA the bath contained 1 μM ionophore, no added Ca^{2+}, and 1 mM $[EGTA]_o$. Breaks in the current trace represent acquisition of current voltage relations.

Source of mobilized calcium

The lack of response of BAPTA-loaded cells to neurotensin suggests that the agonist-induced Ca^{2+} peak results from intracellular Ca^{2+} release. This is also supported by results obtained with the use of nominally Ca^{2+}-free bath solutions. The peak $[Ca^{2+}]_i$ response elicited by neurotensin in cells preexposed (1–5 min) to a nominally Ca^{2+}-free bath (no added Ca^{2+}) was not significantly different from that observed with 1 mM $[Ca^{2+}]_o$; mean = 799 ± 395 nM (n = 9). However, the steady-state $[Ca^{2+}]_i$ was reduced from 68 ± 17 to 56 ± 20 nM (paired experiments, n = 9). Return of $[Ca^{2+}]_i$ to normal resting values did not occur without re-addition of bath calcium. Whole-cell current amplitude was, likewise, reduced by this drop in steady-state $[Ca^{2+}]_i$ but recovered to resting values on restoration of extracellular Ca^{2+}. When cells were preincubated in Ca^{2+}-free solutions (no added calcium, 0.5 mM EGTA) for 30 min, the agonist-induced $[Ca^{2+}]_i$ peak was often abolished, probably due to depletion of the agonist-sensitive cellular Ca^{2+} pool.

As discussed previously, sustained increases in $[Ca^{2+}]_i$ and cell currents often followed the neurotensin-induced peak responses; however, these sustained agonist effects were variable in size and present in only 60% of cells bathed in 1 mM $[Ca^{2+}]_o$. Increasing bath $[Ca^{2+}]$ to 10 mM consistently produced sustained agonist-induced $[Ca^{2+}]_i$ rises—with imaging alone $\{[Ca^{2+}]_i = 226 \pm 104$ nM (n = 13)$\}$ or in combination with whole-cell recording $\{[Ca^{2+}]_i = 332 \pm 165$ nM (n = 5)$\}$. These findings indicate that neurotensin promotes Ca^{2+} influx from the bath and that this accounts for the sustained $[Ca^{2+}]_i$ rise. In the absence of agonist, exposure to 10 mM $[Ca^{2+}]_o$ had no significant effect on $[Ca^{2+}]_i$ (n = 7).

The experiment shown in Figure 8 illustrates the two sources of agonist-evoked Ca^{2+} mobilization. In nominally Ca^{2+}-free media, addition of neurotensin produced a transient rise in $[Ca^{2+}]_i$ from 90 to 450 nM. This was accompa-

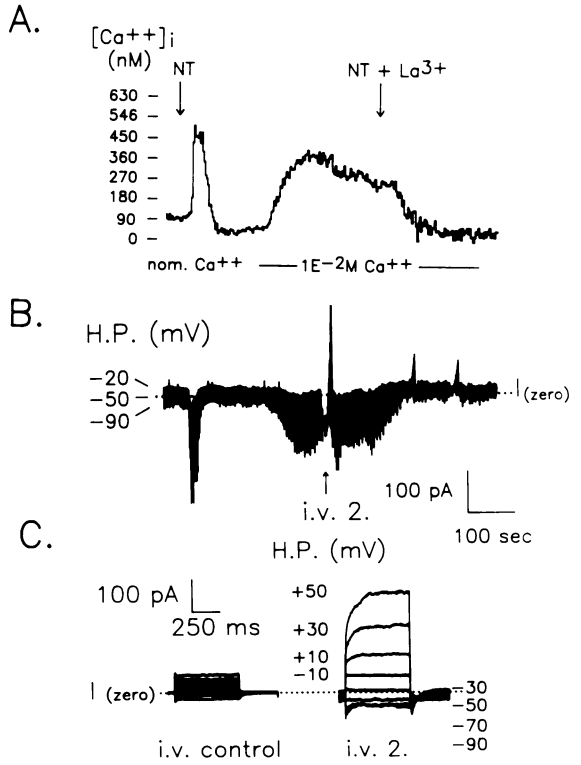

Figure 8. **Effect of neurotensin on $[Ca^{2+}]_i$ and whole-cell currents in nominally Ca^{2+}-free solution.** (A) $[Ca^{2+}]_i$ and (B) whole-cell current record during addition of 5×10^{-8} M neurotensin to a nominally Ca^{2+}-free bath solution (no added Ca^{2+}). During the time shown, $[Ca^{2+}]_o$ was raised to 10 mM (NT still present); subsequently, 100 μM La^{3+} was added to the bath. (C) Current-voltage relations acquired before NT addition (i.v. control, not shown in B) and during the sustained $[Ca^{2+}]_i$ rise (i.v.2.); pulse protocol as in Figure 5.

nied by an increase in inward Cl^- current from 80 to 230 pA. After the peak responses, $[Ca^{2+}]_i$ and Cl^- current recovered to below prestimulation levels. In the continued presence of agonist, addition of 10 mM $CaCl_2$ to the bath evoked increases in $[Ca^{2+}]_i$ and Cl^- current to sustained values of 270 nM and 130 pA, respectively. Subsequent addition of 100 μM lanthanum to the bath inhibited the sustained phases of $[Ca^{2+}]_i$ and Cl^- current stimulation (n = 3). Effects similar to those produced by La^{3+} were seen on removal of neurotensin (n = 2) or depletion of $[Ca^{2+}]_o$ (1 mM bath EGTA) (n = 1). Pretreatment of the cell with 100 μM La^{3+} 30 s before agonist addition did not affect the agonist-induced Ca^{2+} transient (n = 4). These results indicate that the initial transient stimulation of $[Ca^{2+}]_i$ and cell current by agonist is due to Ca^{2+} release from intracellular stores, whereas the sustained phase of stimulation requires Ca^{2+} entry from outside via a La^{3+}-blockable pathway. Current-voltage relations acquired during the sustained $[Ca^{2+}]_i$ and current stimulation (i.v. 2, Figure 8B) show outward rectification, time-dependent inactivation of Cl^- currents at hyperpolarizing voltages, and time-dependent activation at depolarizing voltages (Figure 8C).

Discussion

Calcium-sensitive currents in HT-29 cells

Using simultaneous current and fluorescence measurements, we have shown that undifferentiated HT-29 cells express membrane Cl^- and K^+ conductances that are activated by a rise in cellular Ca^{2+}. Activation of the K^+ conductance required a substantial rise in $[Ca^{2+}]_i$ (>800 nM), whereas whole-cell Cl^- currents were sensitive to small (<10 nM) changes in $[Ca^{2+}]_i$ and were reduced under conditions that deplete cellular Ca^{2+}. Thus, HT-29 Cl^- conductance is sensitive to changes in $[Ca^{2+}]_i$ around the resting level.

Neurotensin and Ca^{2+} ionophore evoked large increases in $[Ca^{2+}]_i$ and whole-cell Cl^- and K^+ currents. The properties of the agonist and ionophore-induced Cl^- currents were similar to those observed previously in lacrimal gland acinar cells challenged with carbachol (Marty *et al.,* 1984) or in T84 colonic tumor cells stimulated by Ca ionophores (Cliff and Frizzell, 1990). The Ca-stimulated Cl^- currents in these systems show outward rectification and voltage- and time-dependent kinetics. Currents inactivate during hyperpolarizing voltage pulses and activate during depolarizing voltage pulses (Figures 5A and 8C).

Calcium mobilization in HT-29 cells

Calcium release from intracellular pools. Ca^{2+} mobilizing receptor stimulation has been correlated with phosphatidyl inositol bisphosphate (PIP_2) breakdown and the generation of inositol polyphosphates and diacylglycerol (DAG) within cells (Berridge and Irvine, 1984). There is now a well-established second-messenger role for 1,4,5-inositol trisphosphate ($InsP_3$) in stimulating Ca^{2+}-sensitive ionic conductances in a variety of cell types. Likewise, a growing body of evidence indicates that the other product of PIP_2 breakdown, DAG, also has second-messenger effects; often these complement or antagonize the effects of Ca^{2+} (for review, see Berridge, 1987).

Neurotensin stimulates PIP_2 breakdown in HT-29 cells (Amar *et al.,* 1986). The Ca^{2+}-mobilizing effects of neurotensin are confined initially to release from an intracellular Ca^{2+} pool. Removal of extracellular Ca^{2+} did not alter the onset, duration, or magnitude of the transient $[Ca^{2+}]_i$ peak or the corresponding whole-cell current response. Additional proof that the initial phase of stimulation depends on intracellular Ca^{2+} release is provided by experiments conducted in cells loaded with the Ca^{2+} chelator BAPTA. BAPTA abolished both the current and $[Ca^{2+}]_i$ responses to neurotensin. Other signal transduction pathways are not involved in the response of HT-29 cells to neurotensin, which stimulates PIP_2 breakdown without changing cAMP or cGMP levels (Laburthe *et al.,* 1978; Amar *et al.,* 1986).

$[Ca^{2+}]_i$ recovery. After the agonist-induced Ca^{2+} peak, both plasma membrane and internal membrane Ca^{2+} pumps are activated to lower $[Ca^{2+}]_i$ (Rink and Sage, 1987; Muallem *et al.,* 1988). The Ca^{2+} pumps involved in Ca^{2+} extrusion and reuptake into cellular pools compete with Ca^{2+} entry and release pathways to determine the time course of $[Ca^{2+}]_i$ during the recovery phase. Evidence that processes for Ca^{2+} extrusion/reuptake are involved in the recovery of $[Ca^{2+}]_i$ is illustrated by the finding that cells often re-adjusted their Ca^{2+} and whole-cell currents to below prestimulus levels after the initial peak values. This undershoot was best observed in cells freshly loaded with fura-2. At later times, presumably when the Ca^{2+} extrusion/reuptake processes were metabolically compromised, $[Ca^{2+}]_i$ recovered more slowly, and the undershoot of $[Ca^{2+}]_i$ and current below basal values was absent (Figure 3).

Ca^{2+} entry and its relation to the intracellular Ca^{2+} pool. Agonist-induced Ca^{2+} influx from the bath followed intracellular Ca^{2+} release. In Ca^{2+}-

free solutions, Ca^{2+} entry cannot compete with Ca^{2+} extrusion/reuptake processes, and $[Ca^{2+}]_i$ falls below resting values (Figure 8). Re-addition of Ca^{2+} to the bath results in a large $[Ca^{2+}]_i$ rise, which can be blocked by La^{3+}. These results reflect the presence of an agonist-stimulated Ca^{2+} entry process, which is responsible for the sustained phase of agonist stimulation in HT-29 cells and a variety of other cell types (Pandol *et al.,* 1987). The $[Ca^{2+}]_i$ and current levels obtained during the sustained phase depend on the interplay between Ca^{2+} entry and extrusion/reuptake processes.

The largest sustained rises in both $[Ca^{2+}]_i$ and current were seen on re-addition of Ca^{2+} to a nominally Ca^{2+}-free bath during agonist stimulation (Figure 8). These results are in keeping with Putney's original observation that depletion of the agonist-sensitive Ca^{2+} pool leads to an enhanced influx of Ca^{2+} across the plasma membrane (Putney, 1986; Takemura and Putney, 1989). This La^{3+}-sensitive Ca^{2+} entry was detected as a sustained rise in $[Ca^{2+}]_i$ that correlated well, in time, with the corresponding elevation in Ca^{2+}-sensitive Cl^- current (see below).

The remainder of the discussion will focus on temporal comparisons between Cl^- currents and $[Ca^{2+}]_i$ afforded by these simultaneous recordings. We will discuss the implications of these measurements for receptor-activated Ca^{2+} signaling pathways and the identification of an inhibitory pathway that is involved in the recovery of Cl^- currents after the $[Ca^{2+}]_i$ rise.

Timing between Cl^- current activation and Ca^{2+} mobilization

Ca^{2+} release. The simultaneous recording of current and $[Ca^{2+}]_i$ demonstrates that the generalized cellular $[Ca^{2+}]_i$ rise induced by neurotensin lags behind Cl^- current activation. This offset in the temporal relations of $[Ca^{2+}]_i$ and current is present under Ca^{2+}-free bath conditions and is, therefore, generated by mobilization of calcium from the agonist-sensitive Ca^{2+} pool. Conventional microelectrode measurements performed in parotid acinar cells have uncovered a similar time dependence in the action of muscarinic agonists on membrane potential and $[Ca^{2+}]_i$ (Foskett *et al.,* 1989). In contrast to the agonist responses, rises in Cl^- current and $[Ca^{2+}]_i$ in response to ionophore were not different in onset (Figure 6), probably because the ionophore rapidly releases Ca^{2+} from *all* internal stores simultaneously (compare Figures 2A and 6Aii).

Indirect evidence supporting a localized release of intracellular Ca^{2+} can be found in studies of a variety of cell types. Density gradient subfractionation of microsomes from epithelial cells of parotid glands indicates that the $InsP_3$-releasable Ca^{2+} pool is found in fractions having a density similar to the plasma membrane (Henne and Soling, 1986). $InsP_3$ binding sites and $InsP_3$-induced Ca^{2+} release have been found in vesicles co-purifying with the plasma membrane of hepatocytes (Guillemette *et al.,* 1988). More recently, $InsP_3$ receptors have been isolated from rat cerebellar membranes (Supattapone *et al.,* 1988) and localized by immunohistochemical techniques to subcellular organelles, mainly within endoplasmic reticulum (ER), nuclear membrane, and cisternae adjacent to the plasma membrane; other cellular organelles were not stained (Ross *et al.*, 1989). Injection of $InsP_3$ below the plasma membrane of *Xenopus* oocytes leads to stimulation of a Ca^{2+}-sensitive Cl^- current. This response is not seen with deeper injections (Busa *et al.,* 1985). In oocytes, a cortical ER, responsive to Ca^{2+}-stimulatory signals, is found close to the plasma membrane (Henson *et al.,* 1989).

The rapid onset of the Ca^{2+}-sensitive Cl^- current evoked by neurotensin in HT-29 cells indicates that $[Ca^{2+}]_i$ mobilization occurs at a site close to the plasma membrane. The initial Ca^{2+} release, resulting from receptor occupancy, PIP_2 breakdown, and the production of $InsP_3$, is monitored by the Ca^{2+}-sensitive plasma membrane Cl^- conductance, with better temporal resolution than that afforded by a measurement of generalized $[Ca^{2+}]_i$ within the cell.

Ca^{2+} entry. When the agonist-induced $[Ca^{2+}]_i$ rise is due to Ca^{2+} entry alone (e.g., Figure 8), there is good temporal agreement between the stimulation of Cl^- current and $[Ca^{2+}]_i$. Why do the time courses of Cl^- current and $[Ca^{2+}]_i$ agree during Ca^{2+} entry but not during Ca^{2+} release? Probably the simplest explanation involves differences in the kinetics of the $[Ca^{2+}]_i$ rises. The rate of $[Ca^{2+}]_i$ rise evoked by agonist-induced Ca^{2+} release is at least an order of magnitude greater than that observed during Ca^{2+} entry (see Figure 8). During this rapid Ca^{2+} release, cytoplasmic Ca^{2+} diffusion is probably the rate-determining step in producing a generalized cellular $[Ca^{2+}]_i$ rise. In contrast, cellular $[Ca^{2+}]_i$ reflects its concentration at the plasma membrane during Ca^{2+} entry because cytoplasmic Ca^{2+} diffusion is not rate limiting. In this context, the process of Ca^{2+} diffusion includes the multiple interactions that Ca^{2+} ions encounter as they move through the cytoplasm.

Recovery of Cl^- currents: an inhibitory pathway

During the transient phase of agonist-induced Ca^{2+} mobilization, Cl^- currents recover toward basal levels before $[Ca^{2+}]_i$ (Figures 3, 6, and 8). At the time of the maximal $[Ca^{2+}]_i$ rise, Cl^- currents had fallen to 65% of their peak value. In contrast, during recovery from the sustained phase of agonist effects, there was not a marked lag between current and $[Ca^{2+}]_i$ (Figure 8). These results can be interpreted in two ways: (a) the Ca^{2+}-sensitive Cl^- current inactivates while Ca^{2+} concentration at the membrane is still high, or (b) the $[Ca^{2+}]_i$ sensed by the channel recovers earlier than the rest of the cell, due to Ca^{2+} extrusion/reuptake processes near the plasma membrane. Image mapping of Ca^{2+} at the $[Ca^{2+}]_i$ peak (7 s, Figure 3C) shows that cytoplasmic $[Ca^{2+}]_i$ is elevated, whereas $[Ca^{2+}]_i$ at the cell periphery is beginning to fall.

Apart from generating $InsP_3$, PIP_2 breakdown also liberates DAG, which is linked to activation of protein kinase C (PKC) (Berridge, 1987). Stimulation of the plasma membrane Ca^{2+} pump and cellular reuptake processes by DAG/PKC pathways (Smallwood *et al.*, 1988; Furukawa *et al.*, 1989) could cause Cl^- currents to recover before $[Ca^{2+}]_i$. Nevertheless, during large agonist-induced $[Ca^{2+}]_i$ responses (e.g., Figure 4), Cl^- currents inactivate even while $[Ca^{2+}]_i$ remains elevated, favoring an inhibitory mechanism. An inhibitory effect of PKC on channel activity at high $[Ca^{2+}]_i$ (Li *et al.*, 1989; Boton *et al.*, 1990) could explain the rapid fall in Cl^- currents that occurs in response to agonist, but not in response to ionophore. This feedback inhibitory pathway would serve to protect cell volume and composition from large Cl^- conductance changes. The possibility that an agonist-mediated inhibitory pathway limits Cl^- conductance changes during a smaller $[Ca^{2+}]_i$ rise (e.g., Figure 3) will require detailed spatial resolution of $[Ca^{2+}]_i$ and Cl^- currents during agonist and ionophore responses.

Methods

Cells

HT-29 cells (ATCC, HTB 38) were grown in McCoy's 5a medium containing 10% fetal bovine serum in a humidified 95% O_2/5% CO_2 atmosphere. Cells were kept in the logarithmic growth phase and were seeded onto sterile collagen-coated coverslips (Fisher Scientific, Springfield, NJ) 4–8 h before use.

Solutions

All solutions were 5 *N*-hydroxyethylpiperazine-*N*-2-ethanesulfonic acid (HEPES)-buffered at pH 7.2. The standard bath solution contained (in mM): 140 NaCl, 4.7 KCl, 1.2 $CaCl_2$, 1 $MgCl_2$, 10 glucose, and 10 HEPES. The standard pipette solution contained (in mM): 80 K glutamate, 40 KCl, 20 NaCl, 1 $MgCl_2$, 10 glucose, and 10 HEPES. Ca^{2+}-free extracellular solutions contained no added calcium and 1 mM EGTA (<10 nM free-Ca^{2+}). Nominally Ca^{2+}-free solutions contained no added calcium (1–5 μM Ca^{2+}). Na^+-free solutions contained NMDG as Na^+ replacement. The osmolarity of these solutions was 290 ± 10 (mean ± SD) mosM. Neuro-tensin peptide and salts were purchased from Sigma (St. Louis, MO).

Fura-2 ratio imaging

A coverslip containing the cells formed the bottom of a nylon experimental chamber. The cells were incubated at 37°C with a 50% mix of culture media and bath solution containing 5 μM fura-2/AM for 30–40 min. For experiments where the intracellular calcium buffering capacity was artificially raised, cells were simultaneously incubated with 10 μM BAPTA/AM (both from Molecular Probes, Eugene, OR). The cells were then washed continuously for the next 20 min and for the duration of the experiment with fresh bath solution. The bath temperature was maintained at 37°C by prewarming the extracellular solutions and by water-jacketing the oil immersion lens of the inverted microscope. Light from a high-intensity-xenon source (XBO 75W, OSRAM, Berlin, FRG) was passed through a digitally controlled electronic shutter/filter changer wheel (Atlantix and Zeiler Instrument, Avon, MA) containing 340- and 380-nm (±10 SD) bandpass excitation filters (OMEGA Optical, Brattleboro, VT) into an IM-35 inverted microscope (Carl Zeiss, Oberkochen, FRG). Excitation light was deflected with a 405-nm dichroic mirror through a 40× oil-immersion lens (Nikon CF fluor, Nikon, Garden City, NY) onto the cells. Emitted light was collected through a 510-nm-long pass emission filter by a high-resolution image intensifier (VideoScope International, Washington, DC) coupled to a video camera (Newvicon@, DAGE MTI, Michigan City, IN). The signal output from the camera was connected to a digital image-processing board controlled by IMAGE1/FL software (Universal Imaging, Media, PA). The average image from eight successive frames was collected and corrected for autofluorescence; then the 340 and 380 nm images were divided on a pixel-by-pixel basis to yield a ratio image. On-line conversion of ratios to $[Ca^{2+}]_i$ was carried out for each cell within the field, using a computer-generated look-up table from the Grynkiewicz formula:

$$[Ca^{2+}]_i = Kd \times (R - R_{min})/(R_{max} - R) \times S_{f2}/S_{b2}$$

where Kd is the dissociation constant for fura-2/Ca^{2+} (224 nM) (Grynkiewicz *et al.*, 1985), R_{min} and R_{max} are determined from in vivo dye calibration as described below, and S_{f2}/S_{b2} is the ratio of excitation efficiencies for free and bound fura-2 recorded at 380 nm. $[Ca^{2+}]_i$ values were collected from measurement windows (~8 × 8 μM) placed in the centers of six cells within the camera field, one of which was used for whole-cell recording (Figure 1A). Cell size varied between 9 and 15 μm. Ratio images were continuously updated every 3.7 s on a color monitor, and the fluorescence output from chosen cells was simultaneously written to hard disk; whole-field images were likewise saved for later analysis. The calibrated, digitized $[Ca^{2+}]_i$ signal from the single cell chosen for whole-cell current recording was passed through a D/A converter (DATA Translation, Marlboro, MA) and displayed in real time on an oscilloscope before being saved on one channel of a PCM/VCR (A.R. Vetter, model 200-T, Rebersburg, PA).

Calibration of the intracellular fura-2 signal

Calibration was performed in vivo with dye-loaded cells bathed in solutions containing ionomycin (1 μM) in the presence of either 10 mM EGTA (R_{min}) or 10 mM $CaCl_2$ (R_{max}). To determine a usable signal-to-noise ratio for the fluorescence signal, the concentration of dye within cells was monitored by comparing the emitted light intensity with that found in solution standards. The excitation wavelength chosen was 358 ± 3 nm, corresponding to the calcium-insensitive (isobestic) point for fura-2. This wavelength likewise indicated cellular dye content during the in vivo calibration. R values were determined from stable maximum changes in emission signal at both excitation wavelengths. Values represent the statistical logarithmatic mean from a large population of cells (n = 1000) for both the Ca^{2+}-free and Ca^{2+}-saturated forms of cellular dye. Using the fura-2/Ca^{2+} dissociation constant reported by Grynkiewicz *et al.* (1985), we found that log $[Ca^{2+}]_i$ was linear over a range of 30 nM–3 μM (the range of $[Ca^{2+}]_i$ encountered in these studies). The optical recording system was linear over the intensity range encountered experimentally; neutral density filters were placed in-line with the excitation filters to produce maximum emission changes within these values. The flatness of the camera field was checked and differences in signal kept within 10% across both the vertical and horizontal axes. Calibrations were performed on a regular basis to account for any spectral changes in light output resulting from burning time of the xenon lamp.

Whole-cell current recordings

Recording electrodes were pulled and fire-polished from KIMAX-51 capillary tubing (Kimble, Toledo, OH) to a resistance of 2–5 MΩ when filled with the standard pipette solution. The perforated patch technique of whole-cell recording (Horn and Marty, 1988) was performed with nystatin from Squibb (New Brunswick, NJ). Whole-cell voltages and currents were recorded using a List EPC-7 patch-clamp amplifier (List-Electronic, Darmstradt, FRG), the output of which was filtered at 1 kHz with an 8-pole Bessel filter (Frequency Devices, Haverhill, MA) before being displayed on the second channel of the oscilloscope and the PCM/VCR. The simultaneous capture of both $[Ca^{2+}]_i$ and whole-cell current signals by the PCM/VCR allowed for later analysis to be carried out without temporal separation. Both signals were also displayed on a chart recorder. Voltage-clamp protocols were generated with the use of P-Clamp software (Axon Instruments, Foster City, CA) and an S-90 stimulator (Medical Systems, Greenvale, NY).

Acknowledgments

We thank Edward C. Walthall for data analysis and assistance with the equipment configuration and Sheila A. Marvin and Ellis P. Bynum for cell culture. This work was supported by the NIH-NIDDK DK31091 and DK38518 and a Fellowship Grant to A.P.M. from the Cystic Fibrosis Foundation.

Received: June 5, 1990.
Revised and accepted: September 12, 1990.

References

Amar, S., Kitabgi, P., and Vincent, J.P. (1986). Activation of phosphatidylinositol turnover by neurotensin receptors in the human colonic adenocarcinoma cell line HT-29. FEBS Lett. *201,* 31–36.

Berridge, M.J., and Irvine, R.F. (1984). Inositol trisphosphate, a novel second messenger in cellular signal transduction. Nature *312,* 315–321.

Berridge, M.J. (1987). Inositol trisphosphate and diacylglycerol: two interacting second messengers. Annu. Rev. Biochem. *56,* 159–193.

Boton, R., Singer, D., and Dascal, N. (1990). Inactivation of calcium-activated chloride conductance in *Xenopus* oocytes: roles of calcium and protein kinase C. Pfluegers Arch. *416,* 1–6.

Busa, W.B., Ferguson, J.E., Joseph, S.K., Williamson, J.R., and Nuccitelli, R. (1985). Activation of frog (*Xenopus laevis*) eggs by inositol trisphosphate. 1. Characterization of Ca^{2+} release from intracellular stores. J. Cell. Biol. *110,* 677–682.

Cliff, W.H., and Frizzell, R.A. (1990). Separate Cl^- conductances activated by cAMP and Ca^{2+} in Cl^--secreting epithelial cells. Proc. Natl. Acad. Sci. USA *87,* 4956–4960.

Dharmsathaphorn, K., Cohn, J., and Beuerlein, G. (1989). Multiple calcium-mediated effector mechanisms regulate chloride secretory responses in T84 cells. Am. J. Physiol. *256* (Cell Physiol. *25*), C1224–C1230.

Fogh, J., and Trempe, G. (1975). New human tumor cell lines. In: Human Tumor Cells in Vitro, ed. J. Fogh, New York: Plenum Press, 115–140.

Foskett, J.K., Gunter-Smith, P.J., Melvin, J.E., and Turner, R.J. (1989). Physiological localization of an agonist-sensitive pool of Ca^{2+} in parotid acinar cells. Proc. Natl. Acad. Sci. USA *86,* 167–171.

Frizzell, R.A., Field, M., and Schultz, S.G. (1979). Sodium-coupled chloride transport by epithelial tissues. Am. J. Physiol. *236* (Renal Fluid Electrolyte Physiol. *5*), F1–F8.

Frizzell, R.A., and Halm, D.R. (1990). Chloride channels in epithelial cells. In: Channels and Noise in Epithelial Tissues. Current Topics in Membranes and Transport, ed. S.I. Helman and W. Van Driessche, New York: Academic Press *37,* 248–281.

Furukawa, K.-I., Tawada, Y., and Shigekawa, M. (1989). Protein kinase C activation stimulates plasma membrane Ca^{2+} pump in cultured vascular smooth muscle cells. J. Biol. Chem. *264,* 4844–4849.

Grynkiewicz, G., Poenie, M., and Tsien, R.Y. (1985). A new generation of Ca^{2+} indicators with greatly improved fluorescence properties. J. Biol. Chem. *260,* 3440–3450.

Guillemette, G., Balla, T., Baukal, A.J., and Catt, K.J. (1988). Characterization of inositol 1,4,5-trisphosphate receptors and calcium mobilization in a hepatic plasma membrane fraction. J. Biol. Chem. *263,* 4541–4548.

Halm, D.R., and Frizzell, R.A. (1990). Intestinal chloride secretion. In: Textbook of Secretory Diarrhea, ed. E. Lebenthal and M. Duffey, New York: Raven Press, chapt. 4, 47–58.

Hamill, O.P., Marty, A.J., Neher, E., Sakmann, B., and Sigworth, F.T. (1981). Improved patch-clamp techniques for high-resolution current recording from cells and cell-free membrane patches. Pfluegers Arch. *391,* 85–100.

Henne, V., and Soling, H.-D. (1986). Guanosine 5′-triphosphate releases calcium from rat liver and guinea pig parotid gland endoplasmic reticulum independently of 1,4,5-trisphosphate. FEBS Lett. *202,* 267–273.

Henson, J.H., Begg, D.A., Beaulieu, S.M., Fishkind, D.J., Bonder, E.M., Terasaki, M., Lebeche, D., and Kaminer, B. (1989). A calsequestrin-like protein in the endoplasmic re-

ticulum of the sea urchin: localization and dynamics in the egg and first cell cycle embryo. J. Cell Biol. *109,* 149–160.

Horn, R., and Marty, A. (1988). Muscarinic activation of ionic currents measured by a new whole-cell recording method. J. Gen. Physiol. *92,* 145–159.

Kitabgi, P., Pastis, C., Granier, C., Van Rietschoten, J., Rivier, J., Morgat, J.L., and Freychet, P. (1980). Neurotensin binding to extraneural and neural receptors: comparison with biological activity and structure-activity relationships. Mol. Pharmacol. *18,* 11–19.

Kopp, R., Lambrecht, G., Mutschler, E., Moser, U., Tacke, R., and Pfeiffer, A. (1989). Human HT-29 colon carcinoma cells contain muscarinic M_3 receptors coupled to phosphoinositide metabolism. Eur. J. Pharmacol. *172,* 397–405.

Laburthe, M., Rousset, M., Boissard, C., Chevalier, G., Zweilbaum, A., and Rosselin, G. (1978). Vasoactive intestinal peptide: a potent stimulator of adenosine 3':5'-cyclic monophosphate accumulation in gut carcinoma cell line in culture. Proc. Natl. Acad. Sci. USA *75,* 2772–2775.

Li, M., McCann, J.D., Anderson, M.P., Clancy, J.P., Liedtke, C.M., Nairn, A.C., Greengard, P., and Welsh, M.J. (1989). Regulation of chloride channels by protein kinase C in normal and cystic fibrosis airway epithelia. Science *244,* 1353–1356.

Marty, A., Tan, Y.P., and Trautman, A. (1984). Three types of calcium-dependant channel in rat lacrimal glands. J. Physiol. *357,* 293–325.

Muallem, S., Pandol, S.J., and Beeker, T.G. (1988). Calcium mobilizing hormones activate the plasma membrane Ca^{++} pump of pancreatic acinar cells. J. Membr. Biol. *106,* 57–69.

Pandol, S.J., Schoeffield, M.S., Fimmel, C.J., and Muallem, S. (1987). The agonist-sensitive calcium pool in the pancreatic acinar cell. J. Biol. Chem. *262,* 16963–16968.

Putney, J.W., Jr. (1986). A model for receptor-regulated calcium entry. Cell Calcium *7,* 1–12.

Reinlib, L., Mikkelsen, R., Zahniser, D., Dharmsathaphorn, K., and Donowitz, M. (1989). Carbachol-induced cytosolic free Ca^{2+} increases in T84 colonic cells seen by microfluorimetry. Am. J. Physiol. *257* (Gastrointest. Liver Physiol. *6*), G950–G960.

Rink, T.J., and Sage, S.O. (1987). Stimulated calcium efflux from fura-2 loaded human platelets. J. Physiol. *393,* 513–524.

Ross, C.A., Meldolesi, J., Milner, T.A., Satoh, T., Supattapone, S., and Snyder, S.H. (1989). Inositol 1,4,5-trisphosphate receptor localised to endoplasmic reticulum in cerebellar purkinje neurons. Nature *339,* 468–470.

Smallwood, J.I., Bruno, G., and Rasmissen, H. (1988). Regulation of erythrocyte Ca^{++} pump activity by protein kinase C. J. Biol. Chem. *263,* 2195–2202.

Smith, P.L., and McCabe, R.D. (1984). A23187-induced changes in colonic K and Cl transport are mediated by separate mechanisms. Am. J. Physiol. *247* (Gastrointest. Liver Physiol. *10*), G695–G702.

Supattapone, S., Worley, P.F., Baraban, J.M., and Snyder, S.H. (1988). Solubilization, purification, and characterisation of an inositol trisphosphate receptor. J. Biol. Chem. *263,* 1530–1534.

Takemura, H., and Putney, J.W., Jr. (1989). Capacitative calcium entry in parotid acinar cells. Biochem. J. *258,* 409–412.

Turner, J.T., and Bollinger, D.W. (1989). Regulation of the neurotensin receptor and calcium mobilization in HT-29 cells. FASEB J. *3,* A1292.

Wong, S.M.E., Linderman, R.P., Parangi, S., and Chase, H.S., Jr. (1989). Role of calcium in mediating action of carbachol in T84 cells. Am. J. Physiol. *256,* (Cell Physiol. *26*), C976–C985.